Marine Physical Laboratory

Analytic Support of the Phillips Lab Whole Sky Imager, 1997-2001

Janet E. Shields, Monette E. Karr, Art
R. Burden, Richard W. Johnson, and
Justin G. Baker

Final Report

August 2002

University of California, San Diego
Scripps Institution of Oceanography

20040809 081

REPORT DOCUMENTATION PAGE

1. Agency Use Only (Leave Blank).	2. Report Date. August 2002	3. Report Type and Dates Covered. Final Report

4. Title and Subtitle.

Analytic Support of the Phillips Lab Whole Sky Imager, 1997-2001

5. Funding Numbers.

N00014-97-C-0385

6. Author(s).

Janet E. Shields, Monette E. Karr, Art R. Burden, Richard W. Johnson, and Justin G. Baker

Project No.
Task No.

7. Performing Monitoring Agency Names(s) and Address(es).

University of California, San Diego
Marine Physical Laboratory
Scripps Institution of Oceanography
San Diego, California 92152

8. Performing Organization Report Number.

9. Sponsoring/Monitoring Agency Name(s) and Address(es).

Office of Naval Research
Ballston Centre Tower One
800 North Quincy Street
Arlington, VA 22217-5660
    CDR Scott Tilden, ONR 321OA

10. Sponsoring/Monitoring Agency Report Number.

11. Supplementary Notes.

12a. Distribution/Availability Statement.

12b. Distribution Code.

13. Abstract (Maximum 200 words).

During this time, repairs were performed as needed, and software upgrades were delivered. A means of providing a very accurate assignment of the angular location (in object space) of each pixel (in image space) was developed and delivered. A first generation night algorithm, for identifying the presence of clouds in a starlight image, was developed. Preliminary work toward extending these technique toward determination of earth-to-space beam transmittance was begun, and is continuing under follow-on funding. This work has enabled the Air Force to continue many productive years of using the WSI in a variety of test-support scenarios.

14. Subject Terms.

whole sky imager, night cloud algorithm development

15. Number of Pages.
28

16. Price Code.

17. Security Classification of Report. Unclassified	18. Security Classification of This Page. Unclassified	19. Security Classification of Abstract.. Unclassified	20. Limitation of Abstract. None

Analytic Support of the Phillips Lab Whole Sky Imager, 1997 - 2001

Janet E. Shields, Monette E. Karr, Art R. Burden,
Richard W. Johnson, and Justin G. Baker

1. Introduction

The Atmospheric Optics Group at the Marine Physical Lab, Scripps Institution of Oceanography, University of California San Diego, has been developing Whole Sky Imagers (WSI) for many years (Johnson 1989, 1991). A Day/Night WSI which had 24-hour a day capability was initially developed in the early 1990's, and further developed since that time (Shields 1993, 1998). One of these instruments, Day/Night WSI Unit 5, was delivered to the Air Force Phillips Lab in December 95. This work was funded under Contract N00014-93-D-0141 DO #11 (Shields 1997a).

A follow-on contract, N00014-96-D-0065-D3 (Shields 1997b) was funded to support additional documentation and to support enhancement of the software provided with the instrument. Under that contract, a new Operations Manual and Theory of Operations Manual were delivered, and the archival and communications software was upgraded to enable several new control options.

This report documents the work that was performed under a second follow-on contract, Contract N00014-97-C-0385, which was funded from July 97 through June 01 for a total of $103,073. This contract was intended to provide support for additional upgrades to the system software, algorithms, and hardware, on an as-needed basis. The work was supported by the Air Force Phillips Lab, later renamed Air Force Research Lab. The Statement of Work is given in Section 2. The initial work, to provide software upgrades and hardware repairs, is discussed in Section 3. Much of the funding increment was used to develop a first-generation night cloud algorithm, as discussed in Section 4. Other software and hardware enhancements performed during the period when the algorithm was under development are discussed in Section 5. The final funding under this contract was used primarily to calibrate the camera in preparation for development of transmittance algorithms. This calibration work is discussed in Section 6, which also provides an overview of ongoing work continuing under other more recent contracts.

Although we normally do not have access to the site and experiments where the instrument is located, our sponsor described the use of the instrument as follows: Air Force Research Laboratory employs the Whole Sky Imager in the role of test support to multiple, high-value experiments. WSI images are displayed on web pages in the test control center to increase situational awareness. WSI data are provided for both daytime and nighttime operations. During certain tests, the test director will use the Whole Sky Imager to either continue, or cancel, the test based on the WSI cloud detection algorithm and resulting picture. AFRL has supported continued algorithm development for increased situational awareness during testing and collection of atmospheric data for post processing.

2. Statement of Work

The Statement of Work from the proposal is as follows:

The contractor shall, unless otherwise specified herein, supply the necessary personnel, facilities, services, and materials to accomplish the following tasks within a two year period following receipt of funding.

a. Coordinate with the sponsor regarding the most appropriate tasks and estimated costs for development.

b. Provide personnel trained in the Whole Sky Imager and its capabilities to address these tasks (at MPL) to the limit of funding provided under the contract. These tasks may include analysis, software development, documentation, minor hardware development, and other tasks related to the WSI which are mutually agreed by the sponsor and by MPL to be appropriate.

c. Provide a final written report and interim verbal reports to the sponsor regarding the results of the above work.

This work was all completed in a timely manner, i.e. using a schedule which best fit the needs of the sponsor. The tasks were discussed in phone communications and visits during the period. The agreed-upon tasks are discussed in the following sections. Interim reports were provided in the form of memos, phone discussions, and e-mail. This written report completes the final requirement. To the best of our knowledge, the funded work has been completed to the satisfaction of the sponsor.

3. Initial Software Enhancements and Hardware Repairs, Jul 97 – May 98

The initial funding increment of $10k was received approximately Jul 97, and followed by $20k in approximately Oct 97. As agreed with the sponsor, these funds were used to further develop the software and to repair the camera.

First, the program View16 was provided in order to enable easier viewing of the WSI images. This program also allowed the user to save 16 bit images as a TIFF image. As documented in Technical Memo AV98-011t (Karr 1998a), an upgrade to the software that runs the WSI, RunWSI, was delivered in Feb 98. This upgrade fixed a subtle problem between the system clock and the WWV clock that was occasionally causing problems. In addition, three "hot keys" were added for more convenient changes in the operational parameters during the program usage. Later upgrades funded under the later funding increments are discussed in Section 5.

Late in 1997, the Photometrics Series 200 16 bit digital camera, which is at the core of the Day/Night WSI, failed. We determined that this was caused inside the Photometrics camera head, by corrosion of the metal surrounding the coolant path. This allowed

coolant to enter the chamber containing the camera CCD and the electronics, all of which were destroyed. Under this contract, a new CCD chip was purchased, and CCD and electronics were replaced by Photometrics. (This required separating the fiber optic taper from the original CCD and bonding it to the new CCD.) The full camera assembly (built by MPL to hold the camera and the optics) was then reassembled, and the camera was recalibrated and returned to the field. This repair was documented in Technical Memo AV97-051t (Shields 1997), which also includes the part numbers of the major components.

The WSI camera housing was reinstalled by Air Force personnel, however some remaining problems resulted in a trip to the site by MPL personnel. We were able to trace the problem to one of the connectors installed by Photometrics during the repair (Wertz, 1998).

4. Night Cloud Algorithm Development Work, May 98 – Mar 00

The next two funding increments, $20k received in May 98 and $40k received in May 99, were intended and used primarily for the work toward a night cloud algorithm, with some of the funding used for hardware support as needed.

The intent of the initial night cloud algorithm is to evaluate all regions of the sky and identify the presence or absence of clouds. (Later algorithms which have been developed or are in development address moonlight conditions and related issues, and should provide optical depth or beam transmittance. Concepts for the development of a higher spatial resolution algorithm have also been developed.) This first algorithm works essentially by evaluating the radiometric signature of the image in the star field. We initially wrote programs to analyze the character of the image near stars, in the presence and absence of clouds. As reported informally in June and July 98 (via e-mail and phone), we evaluated the contrast between a star and its background, and how this contrast changed in the presence of thin clouds. This initial study was sufficiently encouraging to continue the development.

4.1 Initial Star Mapping

In order to automate an algorithm based on star detection, it is necessary to have a means of identifying the expected location of stars in the image. This requires the following:

a) a geometric calibration to convert from zenith and azimuth angle to x,y pixel location.
b) an automated star catalog to provide right ascension and declination of celestial objects
c) a program to derive zenith and azimuth angle of these objects, given the time and location of the WSI, and to convert them into pixel locations in the image

Initial geometric calibration equations were derived from in-house geometric calibrations as documented in Memo AV98-041t (Burden, 1998b). These equations matched the calibration data to within an average error of about .08 degrees or about .2 pixel. For

3

item b, the US Naval Observatory star catalog was chosen (Hoffleit 1991). (This catalog is also known as the National Space Science Data Center star catalog.) This consists of an ASCII file that lists the right ascension, declination, magnitude, and related parameters. A series of programs were written in IDL[1] to derive the positions of the stars in object space and image space, as documented in AV98-041t (Burden, 1998a).

To test the results, a program was written which extracted stars from the star catalog, and plotted squares around the predicted location of stars of magnitude brighter than 4. These were superimposed on a star image. We were reasonably pleased with the results, however this initial geometric calibration was not as accurate as we would like, as documented in Memo AV98-041t. The geometric calibration was refined as discussed in the next section.

4.2 Refining the Star Mapping:

An image of a star in the WSI image plane is typically Gaussian in shape, with a width of 0.5 pixels. That is, the point source in object space is convolved with a roughly Gaussian point spread function due to the atmosphere and the optics in the WSI. Using this information in the image, one can develop more precise techniques for determining the star location. We modified a technique developed by our colleague Dr. Tim Tooman (verbal communication), using Gaussian best-fit routines to determine the sub-pixel location of selected stars. An IDL program was written at MPL, GetStarInfo, which allows one to interactively select stars distributed over the image and then associate each star with a star in the US Naval Observatory catalog. Using this approach, a file is created with the stars' predicted positions in object space and their measured positions in image space.

The known azimuth and zenith angles of 80 to 100 user-selected stars, along with the decimal pixel positions of the stars in the observed image, are then input into a Mathematica[2] program Anglefit written by Dr. Tooman. This program determines an empirical fit between the object space and image space parameters. Use of the program is somewhat complex, and involves an iterative approach, including evaluating the residuals. It is slightly subjective, in that it allows the user to estimate the center position (actually the position on the image corresponding to the zenith), and reruns are made until the user is satisfied with the residuals. Results are typically to within an average error of 0.5 pixels or better. The resulting geometric equations are documented in Technical Memo AV99-043t (Burden 1999a).

---

[1] IDL, which stands for "Interactive Data Visualization", is produced by Research Systems, Inc., which was recently purchased by Kodak. Their address is 4990 Pearl East Circle, Boulder, CO 80301.

[2] Mathematica is produced by Wolfram Research, Inc., whose address is 100 Trade Center Drive, Champaign, IL 61820.

4.3 Development of the Algorithm

The next step in the algorithm development was to develop a program to detect stars in a test image. The program uses the US Naval Observatory star catalog to determine the stars within a selected magnitude range, and predicts their anticipated location in a test image (in image space). The program then finds the largest pixel value within a two-pixel radius of the predicted location. Using a Levenberg-Marquardt best-fit routine[3], the program attempts to fit a two-dimensional Gaussian curve to the data (and in the process determines the true pixel-center of the peak in image space). If the fitting routine gives a reasonable result, the program counts this as a successful detection of the star in the image. Using this technique, we were able to detect most of the stars from magnitude 1 to magnitude 7 in a sample clear image. For example, for zenith angles 30 degrees or less, the program detected 100% of the 33 stars of magnitude 0 to 4, and 88% of the 99 stars of magnitude 0 to 7. For zenith angles of 70 degrees or less, the program detected 78% of the stars of magnitude 0 to 7. Many of the undetected stars were automatically rejected by the algorithm, because it rejects any stars which are near other stars. A test of random locations in an overcast image resulted in a 5% false detection rate.

On the basis of the above results, a first generation cloud algorithm was generated as documented in Technical Memo AV99-044t (Burden, 1999b), which is included in Attachment 1. This program divides the sky out to a 70 degree zenith angle into segments which are approximately 5 degrees in zenith angle by 15 degrees azimuth angle. (Near the center fewer azimuthal segments are made.) This results in 237 regions. Then within each region the program determines whether there are any stars from the star catalog, and if so, determines whether they can be detected simply by the presence of their PSF. The program marks the region grey if there are no candidate stars in the star catalog, blue more than 50% of the available stars in the region are detected, and red if fewer than 50% of the available stars are detected.

This approach worked reasonably well, as shown in the memo. On the clear image, 90% of the regions had candidate stars, and 83% of the regions with candidate stars were identified as clear. The overcast image had a thin overcast; Orion could be seen through the clouds, but most of the dimmer stars could not be seen in the image. In this image, 88% of the regions had candidate stars, and 3% of the regions with candidate stars were identified as clear. The scattered cloud case was in between, with 66% identified as clear.

---

[3] For the LM best fit technique, we used a routine, MPFIT IDL software, written by Craig Markwardt at NASA. It was obtained from Craig B. Markwardt, NASA/GSFC Code 662, Greenbelt, MD 20770, craigm@lheamail.gsfc.nasa.gov, http://cow.physics.wisc.edu/~craigm/idl/idl.html. For a further reference, consider Press, W.H., Et. Al., 1992, Numerical Recipes In Fortran, Cambridge University Press, p. 678-682.

At this point, there were several productive directions we might go in. The decision was made to convert the program in its current (at that time) state to C code, in the hopes of fielding it with the instrument at a later time. Other potential development are discussed in Section 4.5.

4.4. Conversion of the Starlight Algorithm to C

The last step of the algorithm development funded under this contract was the conversion of the code from the interactive IDL code developed as described in Section 4.3 into a more automated C code. This version made more use of input files, as opposed to user input, and was considerably faster (on the order of seconds as opposed to minutes to process an image). This version of the code is documented in Memo AV99-054t (Burden 1999e).

4.5 Further Development of the Starlight Algorithm

Although the sponsor did not have sufficient funds to complete the algorithm in a version which could be fielded with the instrument, this work has been completed under funding from another sponsor. During this later work, the algorithm was also improved considerably in sophistication, to enable it to handle moonlight and, to some extent, nearby city lights.

At present the algorithm is based on uncalibrated raw data. There are several enhancements which should be feasible if using calibrated data, and are invarious stages of development. First, it should be quite feasible to provide estimates of earth-to-space beam transmittance or optical depth. By evaluating the calibrated signal from a large number of stars, and comparing it with the return expected from the stars in the absence of clouds, we feel that we can develop a means for providing a map of the variance in absolute earth-to-space beam transmittance. This work has been funded under a separate contract.

In addition, better handling of moonlight and of city lights should be possible. Our understanding from our sponsors who are using the automated algorithm is that they are quite pleased with the results, but we have not yet done extensive analysis of the results and the potential for improvement.

Also, we have developed approaches for improving the resolution of the night algorithm to potentially provide pixel-by-pixel resolution. While we have not been funded to address this work, we feel that it is a definite possibile future application for the WSI night-time data. An additional useful development would be the application to sunrise and sunset time regimes.

5. Additional Work Performed during the May 98 – Mar 00 Period

Although the funding during this period was primarily directed toward night algorithm development, as discussed in Section 4, additional work to support the ongoing

operational use of the WSI was completed as needed. Another software upgrade was delivered in Oct 98, as documented in Technical Memo AV98-053t and 55t (Karr 1998b and c). This upgrade included addition of a time sync operation that allows the display computer to synchronize with the collection computer. Also, a SCRAMnet life check feature was added to provide a way to check if the SCRAMnet collection is responding. Additional features were added as documented in the tech memo. We also evaluated changes required for Y2K handling and made the necessary changes. An additional minor upgrade is documented in Memo AV99-051t (Karr, 1999).

The sponsor decided that they would like to use the new geometric calibration results to improve the accuracy of the angle assignment to the pixels in the field images. Since Unit 5 is at a classified site, we are restricted from viewing and processing images. For this reason, we developed the geometric calibration procedures into a series of steps that could be performed by the sponsor, and wrote and delivered two tutorial memos documenting these processes. These memos are Technical Memoranda AV99-049t and 050t (Burden, 1999c and d).

A new occultor trolley motor was purchased during this interval, and installed at the site in August 99, as documented in Technical Memo AV99-046t (Wertz and Shields 1999).

6. Preparation for Beam Transmittance Development Work, Mar 00 – Jun 01

The final funds transfer of $13,073 was received approximately Mar 00. At that time, the request was that these funds be saved for camera repair, in case any repair was required. No repairs were required initially. In the meantime, considerable development of the night algorithm occurred under funding from other sponsors, with the result that the night algorithm was fielded on other Day/Night WSI units. Following meetings with the sponsor in October 00, the decision was made to fund the enhancement of the night algorithm to determine earth-to-space beam transmittance. This task was funded under a follow-on contract, N-00014-01-D-0043 DO #5. Development of the beam transmittance algorithm would require calibration of the camera, so the remaining funds under the existing contract were used to acquire the radiometric calibration data for the camera. The camera was also repaired at this time, as documented in Memo AV01-040t (Baker, 2000). Initial work on the calibration processing was also begun, and although the calibration processing was completed under the follow-on contract, the calibration memos AV01-071 – 079 are referenced here. Work on the beam transmittance development is in progress at this time, under the follow-on contract.

7. Summary

The raw WSI night imagery provides extremely useful images, which are easily interpreted by human users. As may be seen from the sample images in the attachment, both clouds and stars can be readily seen, and the general character of the clouds is readily observed. To the best of our knowledge, there is no other instrument in existence, which has this combination of features, allowing human interpretation of the cloud scene during night-time, daylight, and in sunrise and sunset time regimes. In addition, because

7

the data have excellent dynamic range and low noise, and can be calibrated for absolute radiance, they are very useful for further mathematical evaluation. The starlight algorithm is an example of a first-generation algorithm which starts to utilize this outstanding data.

During the period from July 97 through June 01, Contract N00014-97-C-0385 provided funding to support the use of the Day/Night Whole Sky Imager by Air Force Phillips Lab (later renamed Air Force Research Lab). The sponsors were very happy with the instrument, reporting to us that their program "has been very happy with the WSI system we purchased from MPL a few years back. It is an excellent source of data and is a very reliable system." (personal e-mail). During this time, repairs were performed as needed, and software upgrades were delivered. A means of providing a very accurate assignment of the angular location (in object space) of each pixel (in image space) was developed and delivered. A first generation night algorithm, for identifying the presence of clouds in a starlight image, was developed. Preliminary work toward extending these techniques toward determination of earth-to-space beam transmittance was begun, and is continuing under follow-on funding. This work has enabled the Air Force to continue many productive years of using the WSI in a variety of test-support scenarios.

8. Acknowledgements

9. References

In-house Technical Memorandums available at sponsor's request

Baker, J. G., (2001), "Delivery of Repaired Camera to Air Force Unit 5", Atmospheric Optics Group Technical Memorandum AV00-040t, 29 May 00.

Burden, A. R., (1998a), "IDL Software for Converting between Image Pixel Coordinates and Equatorial Coordinates", Atmospheric Optics Group Technical Memorandum AV98-040t, 5 Aug 98.

Burden, A. R., (1998b), "Models from Geometric Calibration of WSI Unit 4", Atmospheric Optics Group Technical Memorandum AV98-041t, 5 Aug 98.

Burden, A. R., (1999a), "Application of ARM Image Geometric Calibration Technique to SGP Data", Atmospheric Optics Group Technical Memorandum AV99-043t, 16 Aug 99.

Burden, A. R., (1999b), "Preliminary Results of Starlight-Based WSI Cloud Algorithm", Atmospheric Optics Group Technical Memorandum AV99-044t, 17 Aug 99.

Burden, A. R., (1999c), "Instructions for Using GetCalibStars: Geometric Calibration Step I", Atmospheric Optics Group Technical Memorandum AV99-049t, 20 Sep 99.

Burden, A. R., (1999d), "Instructions for Using AngleFit: Geometric Calibration Step II", Atmospheric Optics Group Technical Memorandum AV99-050t, 20 Sep 99.

Burden, A. R., (1999e), "GetStarData1 – Conversion to C and Updated Algorithm", Atmospheric Optics Group Technical Memorandum AV99-054t, 15 Dec 99.

Burden, A. R., (2001a), "Basic Geometric Calibration of WSI Unit 5v3", Atmospheric Optics Group Technical Memorandum AV01-071t, 25 Jul 01.

Burden, A. R., (2001b), "Unit 5v3 Rolloff Calibration", Atmospheric Optics Group Technical Memorandum AV01-072t, 26 Jul 01.

Burden, A. R., (2001c), "Unit 5v3 Flat Field Calibration", Atmospheric Optics Group Technical Memorandum AV01-073t, 26 Jul 01.

Burden, A. R., (2001d), "Unit 5v3 Linearity and Exposure Calibration Results", Atmospheric Optics Group Technical Memorandum AV01-074t, 19 Jul 01.

Burden, A. R., (2001e), "Unit 5v3 Effective Lamp Irradiance Computation", Atmospheric Optics Group Technical Memorandum AV01-075t, 19 Jul 01.

Burden, A. R., (2001f), "Unit 5 Version 3 Aperture Calibrations", Atmospheric Optics Group Technical Memorandum AV01-076t, 17 Jul 01.

Burden, A. R., (2001g), "Unit 5v3 Acrylic Dome Callibration", Atmospheric Optics Group Technical Memorandum AV01-077t, 19 Jul 01.

Burden, A. R., (2001h), "Absolute Calibration Results for Unit 5, Version 3", Atmospheric Optics Group Technical Memorandum AV01-078t, 17 Jul 01.

Burden, A. R., (2001i), "Unit 5v3 Calibration Summary", Atmospheric Optics Group Technical Memorandum AV01-079t, 26 Jul 01.

Karr, M. E., (1998a), "Air Force RunWSI updates, Version 5.8", Atmospheric Optics Group Technical Memorandum AV98-011t, 17 Feb 98.

Karr, M. E., (1998b), "Updates to Air Force RunWSI - Version 6.0", Atmospheric Optics Group Technical Memorandum AV98-053t, 01 Oct 98.

Karr, M. E., (1998c), "AF RunWSI version 6.0 documentation", Atmospheric Optics Group Technical Memorandum AV98-055t, 07 Oct 98.

Karr, M. E., (1999), "AF RunWSI version 6.1", Atmospheric Optics Group Technical Memorandum AV99-051t, 19 Oct 99.

Shields, J. E., (1997), "Delivery of Repaired Camera to Air Force Unit 5", Atmospheric Optics Group Technical Memorandum AV97-051t, 30 Dec 97.

Shields, J. E., (2000), "Visit Report: Capt. Dan Gisselquist, 27 Oct 00", Atmospheric Optics Group Technical Memorandum AV00-042t, 31 Oct 00.

Wertz, J. L., (1998), "Trip report for Air Force Unit 5, January 5-6, 1998", Atmospheric Optics Group Technical Memorandum AV98-008t, 06 Feb 98.

Wertz, J. L., and J. E. Shields (1999), "Unit 5 Repair of Trolley Drive Trip Report, August 1999", Atmospheric Optics Group Technical Memorandum AV99-046t, 10 Aug 99/9 Jun 00.

General References

Hoffleit E.D., Warren Jr. W.H., 1991, The Bright Star Catalogue, 5th Revised Ed. (Preliminary Version), Astronomical Data Center, NSSDC/ADC

Johnson, R. W., W. S. Hering and J. E. Shields (1989), "Automated Visibility and Cloud Cover Measurements with a Solid-State Imaging System", Marine Physical Laboratory, Scripps Institution of Oceanography, University of California San Diego, SIO 89-7, GL-TR-89-0061, NTIS No. ADA216906

Johnson, R. W., J. E. Shields, and T. L. Koehoer (1991), "Analysis and Interpretation of Simultaneous Multi-Station Shole Sky Imagery", Marine Physical Laboratory, Scripps Institution of Oceanography, University of California San Diego, SIO 91-3, PL-TR-91-2214

Shields, J. E., R. W. Johnson, and T. L. Koehler, (1993), "Automated Whole Sky Imaging Systems for Cloud Field Assessment", Fourth Symposium on Global Change Studies, 17 – 22 January 1993, American Meteorological Society, Boston, MA

Shields, J. E., R. W. Johnson, M. E. Karr, R. A. Weymouth, and D. S. Sauer, (1997a), "Delivery and Development of a Day/Night Whole Sky Imager with Enhanced Angular Alignment for Full 24 Hour Cloud Distribution Assessment", Marine Physical Laboratory, Scripps Institution of Oceanography, University of California San Diego, Report MPL-U-8/97

Shields, J. E., M. Karr, and R. W. Johnson, (1997b), "Service Support for the Phillips Laboratory Whole Sky Imager", Marine Physical Laboratory, Scripps Institution of Oceanography, University of California San Diego, Report MPL-U-10/97

Shields, J. E., R. W. Johnson, M. E. Karr, and J. L. Wertz, (1998), "Automated Day/Night Whole Sky Imagers for Filed Assessment of Cloud Cover Distributions and Radiance Distributions", Tenth Symposium on Meteorological Observations and Instrumentation, 11 – 16 January 1998, American Meteorological Society, Boston, MA

Technical Memorandum   **AV99-044t**
To: Atmospheric Optics Group   17 August 1999
From: A.R. Burden and J.E. Shields
Subject: Preliminary Results of Starlight-Based WSI Cloud Algorithm

This memo describes preliminary work toward developing a nighttime, starlight-based cloud algorithm to be included in the day-night WSI system. Related information regarding automatic detection of stars in nighttime imagery can be found in Tech. Memos AV98-040t, AV98-042t, and AV99-043t.

Background

The day/night WSI has test software capable of detecting clouds at night under full-moon conditions, but no software is available for detecting clouds at night under moonless conditions. We are currently working on development of a moonless night cloud-detection algorithm for use with the WSI. Here, we discuss some initial findings and present a preliminary cloud-detection algorithm written in IDL. The current capabilities of the algorithm are discussed, as well as issues that we feel need further development.

The approach of the initial study has been to rely on the difference in the optical characteristics of a star under cloud-free conditions compared to cloudy conditions. When an image is formed by an optical system, the image is normally slightly defocused. Mathematically, the image is convolved with the point-spread function (PSF) of the optics. For example, the image of a point source, such as a star, may be spread out over several pixels. The PSF for the WSI optical system can be modeled by a Gaussian distribution. Using images of stars, we have found that the width of the PSF, which is equal to the standard deviation of the Gaussian distribution, is typically 0.3-0.8 pixels. It does not appear to vary systematically over the image.

An image of a star centered on a pixel is characterized by a peak signal at the center pixel surrounded by pixels exhibiting signals that decrease to the background value further from the peak. A star with a point-spread function of 0.5 is characterized by a signal that is reduced to background within three pixels of the center. If the same star is obscured by opaque cloud, most of the signal from the star will not be transmitted through the cloud to the camera. The signal from the cloud will not exhibit Gaussian behavior, and will most likely exhibit only small variations in signal. If the cloud covering the star is semi-transparent, a reduced signal from the star may still show through. The background signal may be increased by the presence of the thin cloud.

Using a star catalog to determine the locations of bright stars within a WSI image, we can search for the stars using tests based on the differences in optical characteristics just described.

The presence of a Gaussian-like peak at the expected star location can be used as an indicator of cloud-free conditions, while the absence of the peak can be used as an indicator of cloud obscuration. This basic feature, along with other tests based on differences in signal for stars and clouds, is incorporated into the first-generation cloud-detection algorithm described below. This scheme represents one possible method for identifying clouds in WSI imagery. Other possible schemes may be considered as funding permits.

The algorithm described here has not been written in a form that is ideal for real-time use with the WSI. Rather, it was written in IDL to facilitate the development of such an algorithm that could later be written in C and incorporated into the field software. The basic structure of the current algorithm can be divided into two parts: subroutines that obtain information about the catalog stars and the image pixels that correspond with these stars, and subroutines that use this information in tests that differentiate cloud-free and cloudy regions.

The first group of subroutines is called by the main routine GetStarData. The IDL version of GetStarData can be very time consuming to run, as it stores data for thousands of stars in an image with magnitudes in the range 0-7. The information from GetStarData is saved in a file for each image, and available for future analysis using the second part of the algorithm. At this time, the cloud decision part of the algorithm is found in a routine called StarAlgorithm1. As new methods of cloud detection are developed, they can be incorporated into the algorithm and applied to GetStarData output files without having to rerun the entire set of procedures.

Data

In order to develop and test the new nighttime algorithm, images have been obtained from an archive of data collected with the WSI located at the SGP site operated by ARM. These images were obtained by contacting the ARM archive and requesting data from several nights without moonlight during the years 1997-1999. The data were downloaded from the ARM archive web site and extracted from compressed archive files. Each image file was then calibrated using the IDL software Wsi_SGP_Data_Ingest, written by Tim Tooman of Sandia National Laboratory, using the radiometric calibration equations developed at MPL. The resulting files are in the NetCDF data format. Files written in the NetCDF format can be read using standard IDL routines. The MPL-written routines GetCDFData and GetCDFDate are used to extract the image and header information for use in the current study.

GetStarData

Locating Star Positions

In order to identify a star in WSI imagery, the theoretical location of the star and a transformation from the theoretical coordinates to image coordinates are required. The first item is easily obtained from one of many bright star catalogs available. Star catalogs, such as the National Space Science Data Center (NSSDC) bright star catalog used here, contain vital information about known stars, including right ascension, declination, magnitude, and reference

numbers. The NSSDC catalog used here is a formatted ASCII file containing over 9100 stars of up to magnitude 8 (magnitude decreases with brightness).

The geometric calibration routine, Rad2Az, described in AV98-040t is used to convert celestial coordinates (right ascension, declination) for a star to spherical coordinates (azimuth, zenith) when the time of observation is known. Although coarse equations to derive pixel locations from spherical coordinates are given in AV98-040t, we now use a more precise geometric calibration based on an empirical best fit that is a function of azimuth and zenith angles to obtain image pixel coordinates. This procedure, described in AV99-043t, is capable of locating stars in the catalog to within half a pixel. The conversion routine that uses the empirical fit equations is called GetStarXY.

The conversion equations obtained with the fitting procedure must be reworked for different WSI cameras and each time a WSI camera is moved. In the case of SGP data, the camera was moved on a couple of occasions during the period of study, December 18, 1997 to January 17, 1999. Therefore, three sets of calibration equations were developed, and the appropriate set is used according the date given in the filename of each image.

Identifying Stars in Cloud-Free Images

Once the position of a star in image pixel coordinates has been determined, the next step is to determine whether a star-like peak exists in the image at that point. For this study, we use an iterative method that searches the region surrounding the calculated star center for a peak. First, the maximum signal for the pixels directly next to and including the calculated star center is determined. If the pixel with maximum signal is the calculated star center, the search is stopped. Otherwise, the pixel with maximum signal is labeled as the new center pixel and the process is repeated. If no star center can be found within a certain pixel distance of the calculated star center, the search is considered a failure. For this study, a maximum distance of three pixels was used. Because crowded star fields may contain multiple star peaks in the same region, a second attempt, more sophisticated attempt, is made to find a different peak near the calculated star center when the first attempt fails. The IDL routine that searches for potential star peaks is called FindCenterPixel.

Fitting Potential Stars to 2-Dimensional Gaussian Distribution

If a potential star peak is found near the calculated star position, a best fit calculation is made using the peak pixel and the surrounding pixels. The best fit subroutine uses the Levenberg-Marquardt method (LMM), which is a robust technique commonly used for solving non-linear least-squares problems (see Numerical Recipes, Press, et al, for instance). Additional information on the method will be documented in a future memo describing software for focusing the WSI camera. The array of pixel values that represents the star are fitted with a two-dimensional Gaussian function with six parameters, as shown in Equation 1. An additional parameter, the tilt, which can be used to determine the orientation of an asymmetrical Gaussian about the axes, has been left out for now. While the asymmetric nature of a star distribution is more realistic, model results to date have not been reasonable.

$$F(x,y) = A_0 + A_1 e^{-\frac{1}{2}\left[\left(\frac{(x-A_4)}{A_2}\right)^2 + \left(\frac{(y-A_5)}{A_3}\right)^2\right]}$$

(1)

with the following parameters:

A_0 = Background value
A_1 = Scaling factor
A_2 = Width of Gaussian in the x-direction (point spread)
A_3 = Width of Gaussian in the y-direction (point spread)
A_4 = Center in x-direction
A_5 = Center in y-direction

LMM finds the set of parameters that best fits the array of pixel values. The fit is "best" in the least-squares sense; that is, the sum of the weighted, squared differences between the model and data is minimized. While calibrated data were used in this case, the routines work similarly for uncalibrated WSI images. The IDL subroutines that perform the best fit calculation are called MPFit and MPFitFun. These subroutines were converted from Fortran routines included in the MinPack statistical package by Craig B. Markwardt of NASA. Additional information can be obtained at his website: http://cow.physics.wisc.edu/~craigm/idl.

As described in the Validation section, the LMM has several optional inputs that may affect the results: an array may be passed to MPFitFun that contains weights for each pixel value; the six parameters can be given constraints on their values; and a ceiling can be put on the number of iterations performed. Additionally, multiple best fit calculations may be required when the original, 5- by 5-pixel array does not provide a good fit. The 1-sigma errors produced by the covariance matrix of the best fit are used as an indicator of good fit, and may be high when the array size is not large enough. When a parameter error is higher than a certain threshold, the fit is considered suspect. In this case, the array width is increased by 2 pixels, and the fit is performed again. A maximum array size of 11 by 11 pixels is used. While somewhat arbitrary, this method has shown to give better results than using either small arrays or large arrays alone. Some stars require additional surrounding pixels to be distinguished from the background, while others lie in crowded star fields where too large an array prohibits a good fit with the Gaussian model.

For each best fit calculation, important information is stored regarding the results. As stated in the previous paragraph, when a best fit calculation results in large error values, a new calculation is made with a larger input array. Other factors that merit a new calculation include iterations that exceed a specified maximum and star point-spread function widths that exceed specified limits. For this study, calculations exceeding 300 iterations or point-spread function widths outside the range 0-2 were performed again with larger arrays. Most best fit calculations converge within a few iterations, especially for brighter stars. If no array width between 5 and

11 pixels results in an acceptable outcome, the star in question is flagged with an appropriate code (Code 1 if maximum iterations or point-spread limits exceeded; Code 4 if large errors) identifying the cause of the failure. Additional flags are set if the region near the calculated star center is potentially crowded with stars (Code 2: multiple peaks nearby), or if the star peak coincides with a previously identified star (Code 3: stars with identical center). All other outcomes are classified as a success (Code 0). The list of MPL-written subroutines used in the best-fit calculation includes CheckForPeak, StarPeak, RunMPFit, and Gauss2D_Mod.

Statistics and Data Storage

The next step after the best fit has been determined is to calculate certain statistics for the star, or lack thereof. The contrast is calculated by finding the integral of the two-dimensional Gaussian model of the star and dividing the result by the background value for the star. The background is just the first parameter resulting from the best fit. The peak is equal to the sum of the background and scaling factor (i.e., $A_0 + A_1$). The full-width-half-maximum (FWHM) is defined for a Gaussian distribution to be $\sqrt{8\ln(2)}\sigma$, or 2.36σ[†]. Since in this case the distribution is two-dimensional, we take the mean of the x and y FWHM values.

For cases where no satisfactory fit was found, the statistics are calculated differently. The background is the median of the 9- by 9-pixel array surrounding the calculated star center. The peak is the mean of the 3- by 3-pixel array surrounding the calculated star center. The contrast is the peak minus the background divided by the background. The FWHM is set equal to 0. The statistical calculation routines are StoreStats and Gauss2Dintegral.

Currently, for each image analyzed, information is recorded for all stars in the NSSDC catalog with magnitudes in the range 0-7 and zenith angles less than 70°. The following information is stored for each star: HR and SAO catalog numbers, right ascension, declination, magnitude, multiple star designation, zenith, azimuth, expected x-pixel, expected y-pixel, image x-pixel, image y-pixel, quality flag, background, peak, contrast, the x and y point-spread functions, and a image cell number described in the next section.

Star Algorithm 1

Below is a description of the preliminary version of the nighttime, starlight-based cloud algorithm based on initial study results. While simple in its application, it demonstrates that the basic concepts described in the previous sections can yield reasonable results. The approach used here is to define a number of regions, or 'image cells', that are approximately the same size and oriented around the image center, as shown in Figure 1. The grid is made up of a total of 237 image cells covering zenith angles up to 70°. Each image cell is examined to determine the number of potential stars that exist there. If at least half the potential stars are identified as exhibiting star-like qualities, the entire image cell is classified as cloud-free.

[†] The Full Width at Half Maximum is the width of the Gaussian distribution at the half-power point, which is equal to 0.5 for a normal distribution. The value shown here is obtained by solving the one-dimensional Gaussian for x and multiplying the result by 2.

Figure 1. WSI Image Overlayed with Cloud Decision Grid
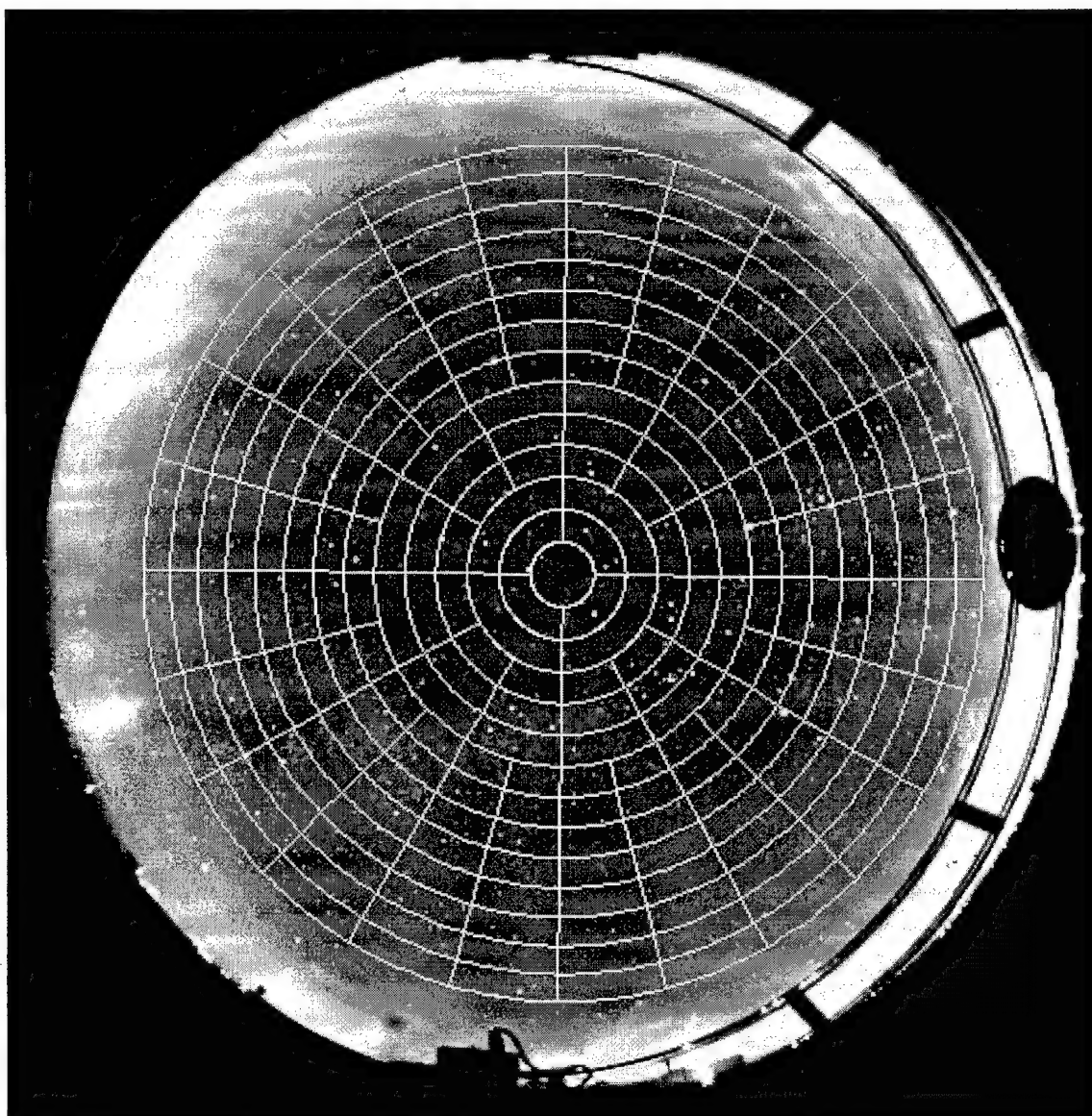
Parameters that are considered important for identifying a star include: the contrast of the star peak with the sky background; the width of the point spread functions associated with the Gaussian model of the star; and the value of the quality flag based on the best fit determination for the star. Additionally, the contrast of a star as well as the ability of the best fit algorithm to successfully converge is diminished for higher magnitude stars. Therefore, the quality flag, contrast, and point-spread functions of low magnitude stars within an image cell are examined first. If none exist, then all other stars are examined. The magnitude threshold used here is 5.

Before the clear and cloudy regions in the image are identified, all stars that were flagged as being stacked on other, lower magnitude stars (Code 3), are removed from the dataset. Each image cell is then categorized as cloud-free or cloudy. The first step of the decision process is to

identify any star in the image cell with Code 1, defined here as a best fit failure, as cloudy. Next, all stars in the image cell with a contrast >0.18 and x- and y-point spread function widths in the range 0.3-0.8 are identified as cloud-free. All other stars in the image cell are classified as cloudy. If the number of cloud-free stars is at least half the total number of low magnitude stars in the cell, the entire cell is identified as cloud-free. If no low magnitude stars are found in the image cell, the same process is done for the high magnitude stars. At this time, the additional information from Codes 2 and 4 is not used.

The thresholds used in the algorithm were obtained by examining the point-spread function widths of stars in completely cloud-free images and by comparing the contrast of stars in completely cloud-free images and completely overcast images. Figure 2 shows the distribution of point-spread functions for stars identified in several cloud-free images. The data were separated into low and high magnitude stars, and stars flagged as having poor best fit convergence were removed from the data. Each distribution was fitted with a Gaussian distribution to estimate the mean and standard deviation. In both cases, the point-spread function widths were centered near 0.48, with most cases being in the range 0.3-0.8. The high magnitude distribution exhibited a slightly lower mean, but skewed toward higher point-spread function widths. This demonstrates the difficulty in performing best fit calculations on high magnitude stars.

Figure 3 shows contrast distributions for stars under cloud-free conditions and stars under cloudy conditions. Again, stars were divided into low and high magnitude datasets. In order to highlight the differences in the distributions, only contrasts up to a value of 5 were plotted. In the cloud-free, low magnitude case, most of the values were in the range 0.25-2.5. A few stars had contrasts as high as 50 or more. The contrasts for the cloud-free, high magnitude case were much lower, with most of the values lying in the range 0.05-1.0. Under completely overcast conditions, the contrasts rarely increase above 0.2, and these cases may be due to optical aberrations, bright stars being viewed through clouds with lower optical depth, or natural variations in cloud radiance. Since some crossover exists between the cloud-free and overcast distributions, the results of the cloud decision algorithm will be dependent on how the threshold is applied. In this case, a threshold of 0.18 will misidentify some potentially cloud-free stars as being obscured by clouds. Since the number of cases that fall into that range appears small, the results should not be drastically affected.

Algorithm Results and Validation

When GetCloudData is run, several optional parameters may be included in the calculation of the LMM best fit. Results to date show that there is some dependence of the results on how these parameters are initialized. For instance, an array input to MPFit contains limits for each of the six parameters. Preliminary studies showed that limiting the point-spread function widths had an adverse affect on the results. Therefore, requiring that the background and scaling factors be greater than zero were the only limits used.

It was also found that the LMM subroutine works best when given initial parameters that are close to the minimized values. The background value is set equal to the minimum pixel value in the input array. The scaling factor is set equal to the maximum pixel value minus the minimum pixel value. The x-and y-widths are equal to 0.5, since this is a typical point-spread function width. Finally, the x- and y-centers are set to the central pixel location.

An additional parameter that needs to be investigated further is the use of weighted pixel values. It has been found that leaving the pixel values unweighted is effective for low magnitude

Figure 2. Point–Spread Function Widths for Cloud–Free Images
Magnitudes < 5 (solid) and Magnitudes > 5 (dash)

Gaussian Fit (M<5):
Mean = 0.482
SDev = 0.083

Gaussian Fit (M>5):
Mean = 0.473
SDev = 0.103

Relative Frequency

Point–Spread Function Width (pixels)
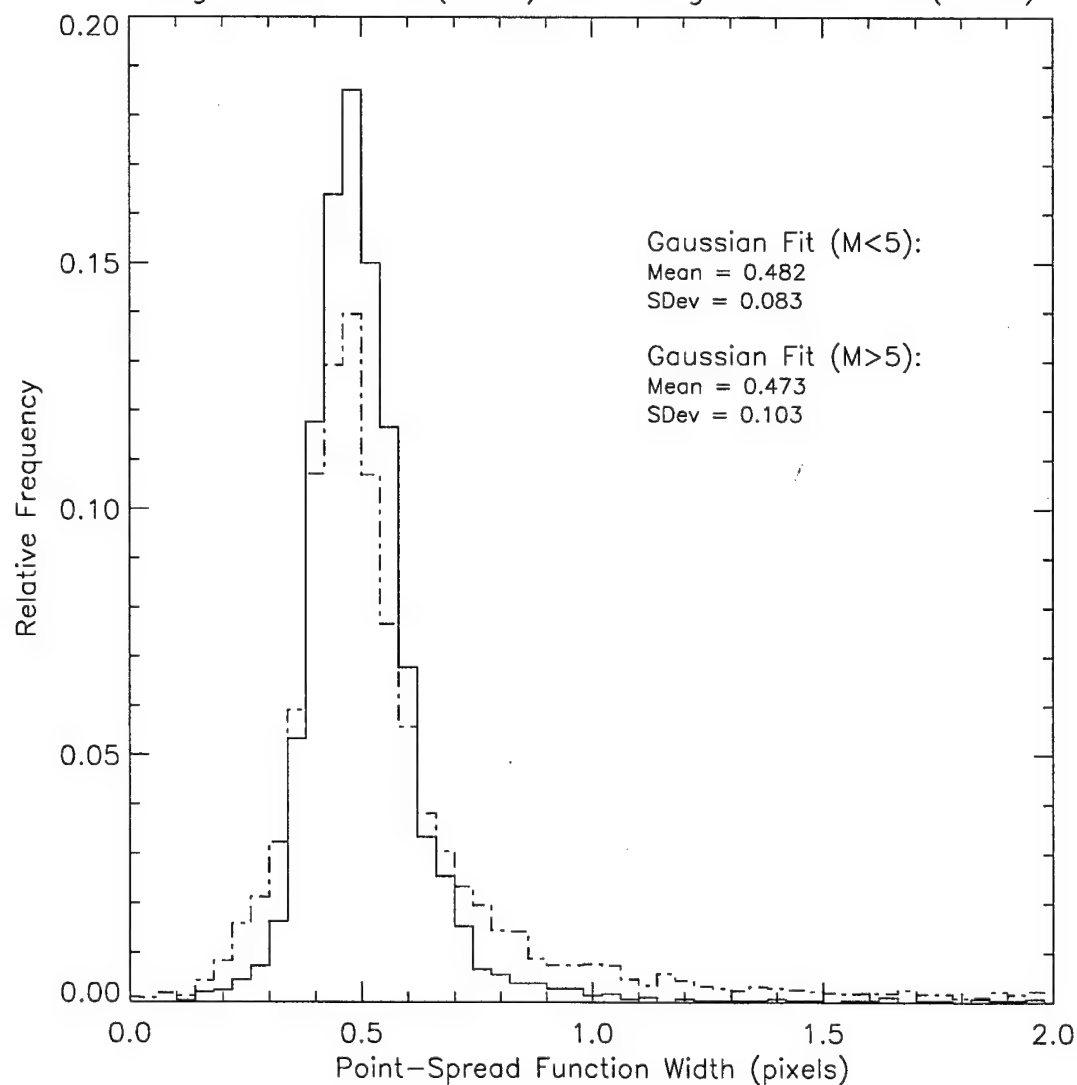
Figure 3. Comparison of Star Contrast for Cloud—Free and Cloudy Conditions
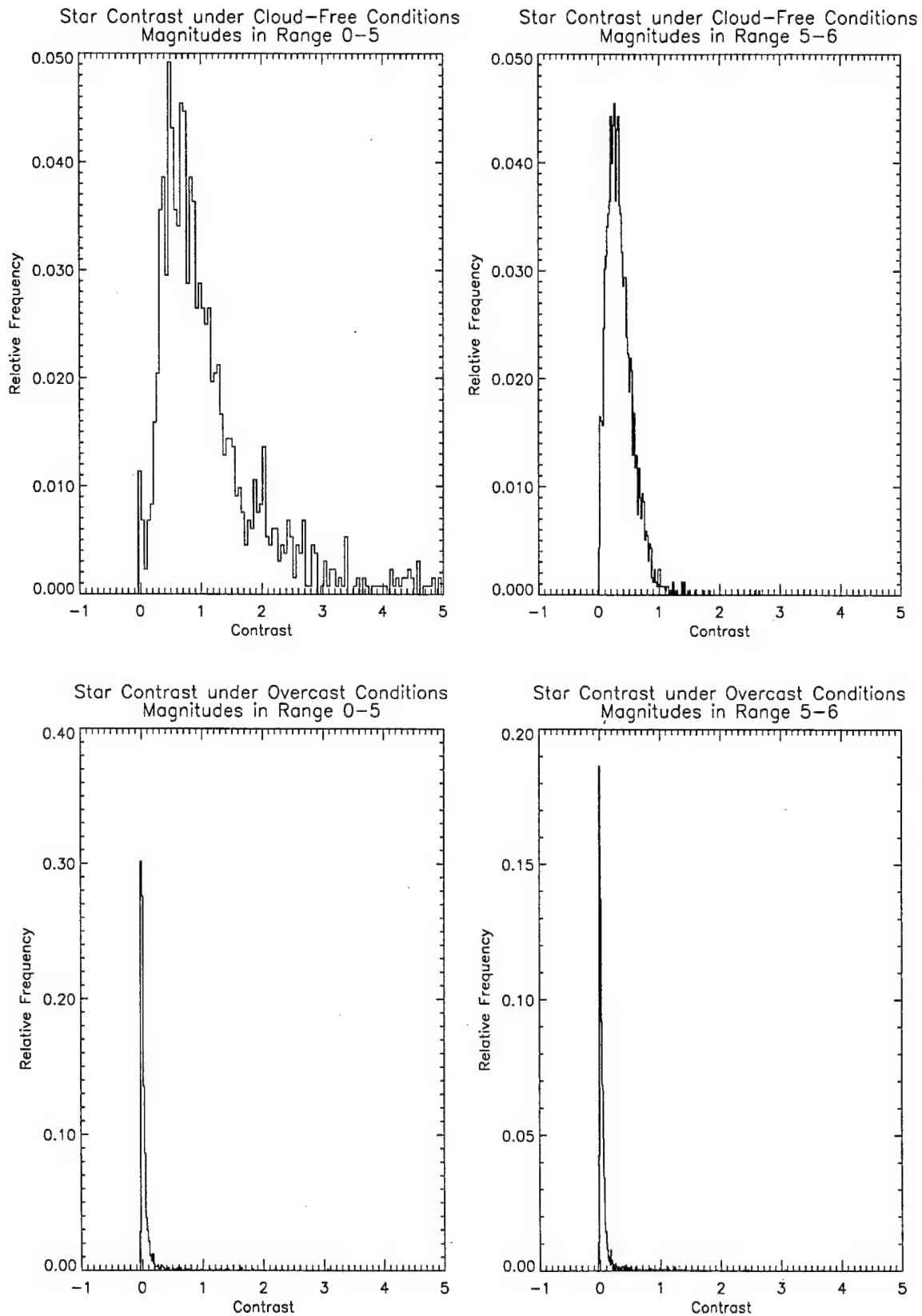
stars, but using weights that are directly proportional to each pixel value is more effective for high magnitude stars. The point-spread functions are more realistic, and the algorithm converges much quicker. One possible scenario is to use unweighted pixel values for low magnitude stars, switching to weights beyond a certain magnitude value. For the data used in this memo, no weights were used.

Despite the large number of dependencies, LMM is quite robust. CURVEFIT, the nonlinear least-squares routine included with IDL, uses a gradient expansion algorithm. A comparison of the two methods using modeled stars in the form of two-dimensional Gaussian distributions showed LMM converged to the exact point-spread function values in most cases, while the gradient expansion method did not. Results for the two methods were comparable when an input array with a width of nine pixels was used, except for point-spread function widths less than 0.4, where LMM results were superior. Neither method worked well when the model star's point-spread function width was much lower than 0.3. When the array width was reduced to five pixels, the gradient expansion method performed far worse than LMM.

To validate the preliminary star algorithm, several nighttime images were analyzed. Figures 4 to 8 each show the original image and the image overlaid with a mask that is color-coded to represent the cases of cloud-free (blue), overcast (red), and no usable stars (gray). The first two examples are cloud-free images collected at 0427 UT on December 18, 1998 and 0220 UT on December 18, 1997, respectively. Figures 6 and 7 are of completely overcast images collected at 0356 UT on November 18, 1998 and 0820 UT on January 17, 1999, respectively. Finally, Figure 8 shows an image partly covered with thin and opaque clouds collected at 1127 UT on December 18, 1998.

Table 1 summarizes the number of image cells out of 237 that fall into each category. Also shown is the number of image cells that did not have any stars with magnitudes <5. While the results are not perfect, the overall strategy appears to be effective.

Table 1.
Number of Image Cells in Each Category

Image	Cloud-Free	Obscured by Cloud	No Stars	# w/o Low Mag Stars
Cloud-Free 1	228	8	1	38
Cloud-Free 2	230	7	0	35
Overcast 1	3	234	0	34
Overcast 2	1	235	1	41
Partly-Cloudy	28	206	3	37

We can also examine the results by looking at the stars individually. Table 2 gives the algorithm results for catalog stars as a function of magnitude and zenith angle. The data is

summarized from multiple cloud-free images. The first column lists the magnitude range for the row. Results shown in the other columns are broken down by zenith angle: stars with zenith angles less than 70, 50, and 30°, respectively. The second column shows the total number of catalog stars in the given magnitude range. The third column gives the percentage of peaks identified as catalog stars using the full algorithm logic, including contrast and point-spread width thresholds. The last column shows the mean residual in pixels between the star coordinates found from the Gaussian best fit and the image star coordinates corresponding to the stars identified in column three.

Table 2. Star Identification Results for Cloud-Free Scenes as a Function of
Star Magnitude and Zenith Angle

Magnitude Range	Number of Stars (70/50/30°)	% Success by Zenith Angle (70/50/30°)	Mean Pixel Residual by Zenith Angle (70/50/30°)
0.0-4.0	296 / 168 / 75	0.93 / 0.89 / 0.91	0.48 / 0.37 / 0.31
4.0-5.0	728 / 421 / 175	0.90 / 0.90 / 0.86	0.51 / 0.43 / 0.35
5.0-6.0	2093 / 1164 / 438	0.61 / 0.65 / 0.68	0.58 / 0.49 / 0.43
6.0-7.0	2104 / 1151 / 438	0.25 / 0.30 / 0.30	0.57 / 0.45 / 0.43

It is clear from the table that the number of available stars increases substantially with magnitude. It can also be seen that the ability to successfully identify stars decreases with magnitude. This is not all that surprising, since the fainter stars are not expected to stand out from the background as well as brighter stars, and therefore less likely to be identified with the best fit algorithm. The percentage of identified stars with magnitudes less than 5, 86-93%, is quite good. Beyond that, the percentages drop off substantially, and for magnitudes 6 and greater, the stars appear to be a useless indicator for the methods used here. Looking at the flags that were set for these stars, 30% of magnitude 5-6 stars and 56% of magnitude 6-7 stars had additional peaks nearby. These additional signals undoubtedly contributed to the failure of the best fit algorithm for most of the cases. The residuals shown in the last column increase somewhat with magnitude, but the change is not significant. All cases had mean residuals less than 0.6 pixel.

While there is a finite probability that, given random pixel coordinates, a peak associated with a star will be found nearby, examination of images showing the location of catalog stars and the associated peaks shows that the method works well for low magnitudes. To test the likelihood of randomly finding a peak resembling a star in an image, a routine called GetRandomStars was written. This routine uses a random number generator to obtain dummy star locations that are then passed to the peak search and best fit subroutines, just as with the catalog stars. In the case of completely cloud-free images, there was about 20% chance that a peak resembling a star was located using the star algorithm, given 500 random coordinates. Examining the resulting peak locations showed that the majority of these peaks were indeed stars. The same exercise with a completely overcast image resulted in less than 1% chance that a peak resembling a star was located.

Conclusion and Future Work

This first generation algorithm appears to work well for skies with no moon. There are several approaches to further optimization that we feel would be worth evaluating. One approach that has showed reasonable results involves the ratio between the contrast for a star in a cloud-free image and the contrast for the same star in an unknown image. This method appears to work well in distinguishing cloud-free, thin cloud and opaque cloud in the unknown image. In this case, a library of cloud-free contrast values for specific stars would need to be created. Unfortunately, light from man-made and other sources creates some dependence of the sky background on zenith angle. This dependence must be removed before the contrast ratio method could be applied. In addition, it may be possible to further optimize this algorithm with techniques such as customizing the star list to remove stars that are close to a brighter star. Removing secondary peaks near the star center from the input array may aid in calculating the best fit Gaussian, particularly with high magnitude stars. The algorithm also needs to be evaluated using data from other sites and using raw data as opposed to calibrated data.

However, we feel that this first generation algorithm is sufficiently accurate to merit converting to C-code that can be included in field software. Once a usable field version is written, future developments could include determination of optical depth from the calibrated images, evaluating the transition to partial moonlight, and increasing the angular extent and/or angular resolution of the algorithm.

Figure 4. Cloud—Free Scene
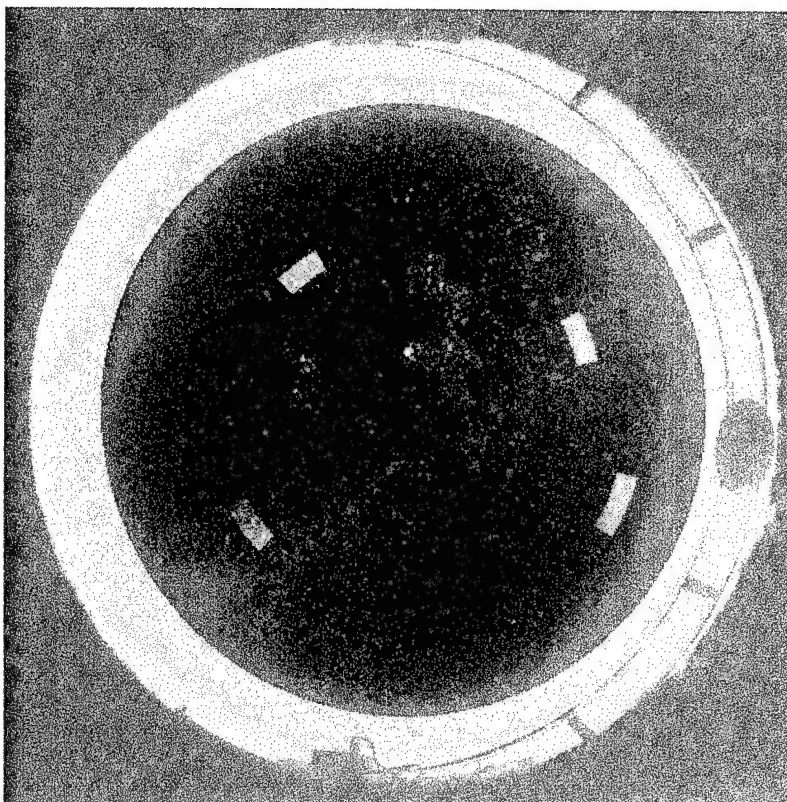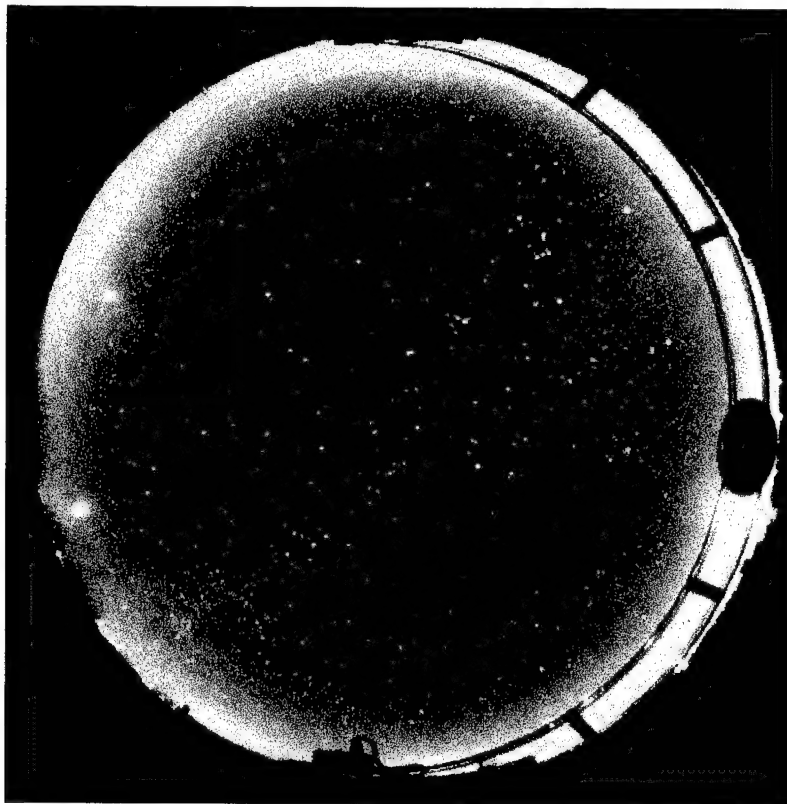Grey = No Stars, Red = >50% Failure, Blue = <50% Failure

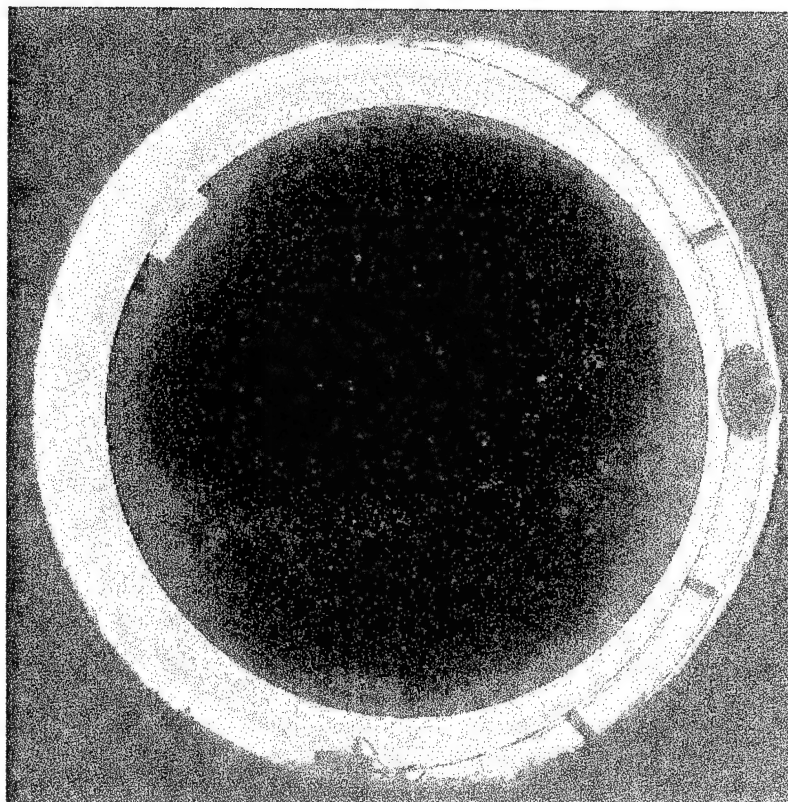Figure 5. Cloud−Free Scene
Red = >50% Failure, Blue = <50% Failure
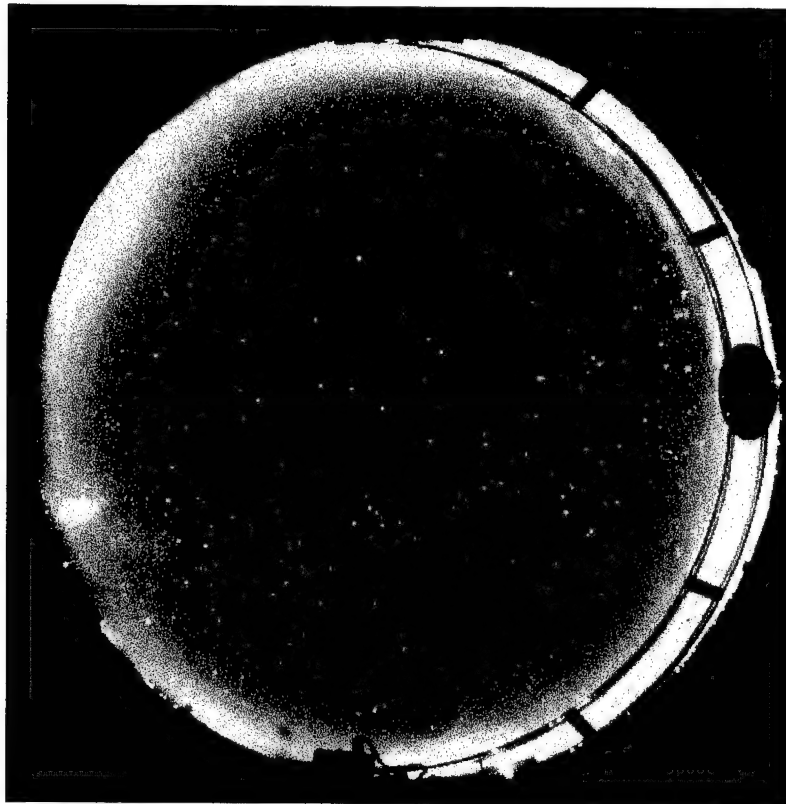
Figure 6. Overcast Scene
Red = >50% Failure, Blue = <50% Failure
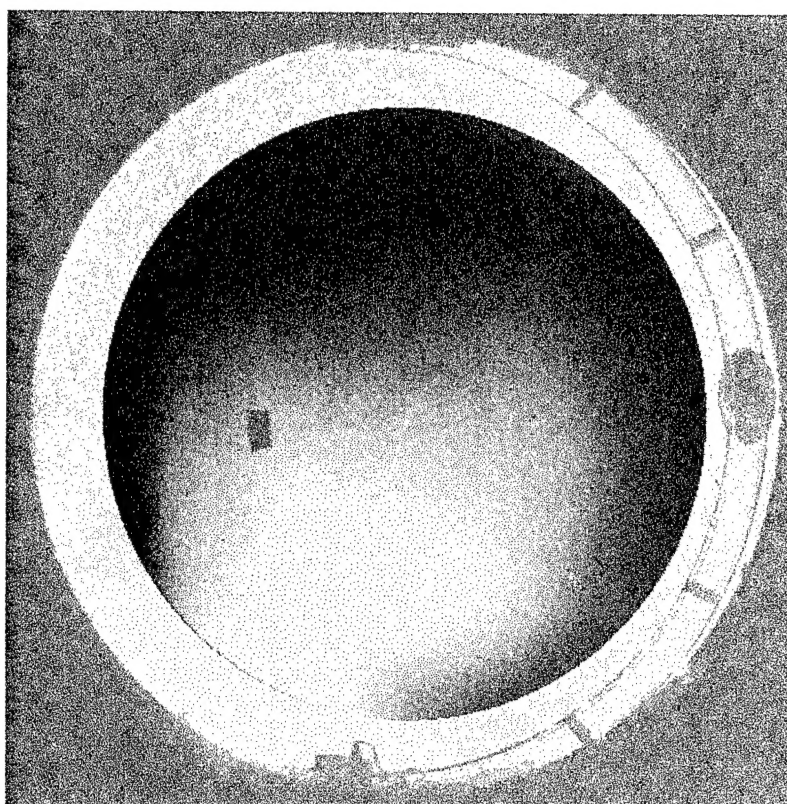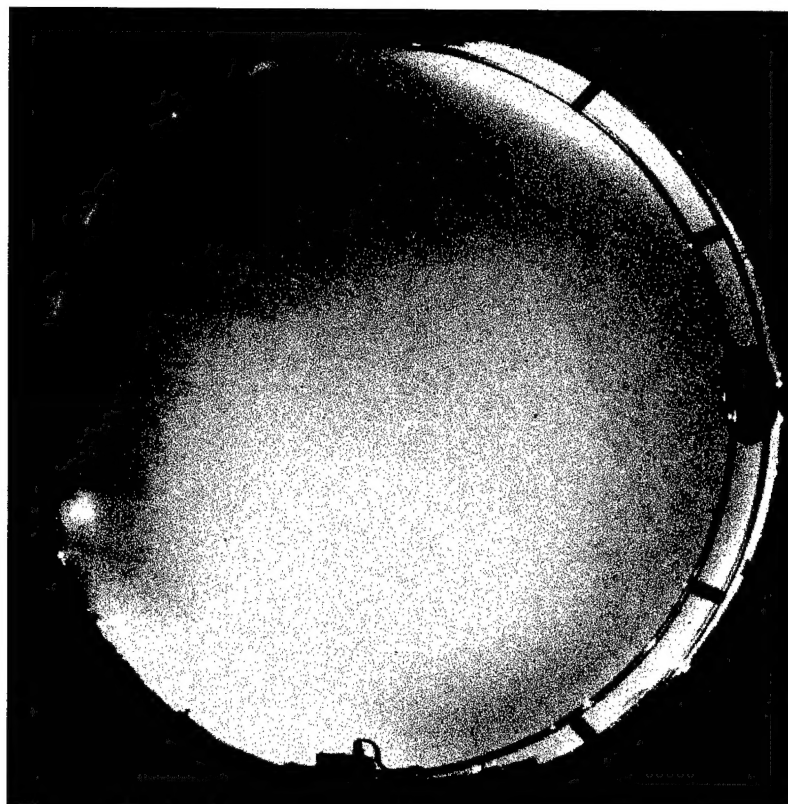
Figure 7. Overcast Scene
Grey = No Stars, Red = >50% Failure, Blue = <50% Failure

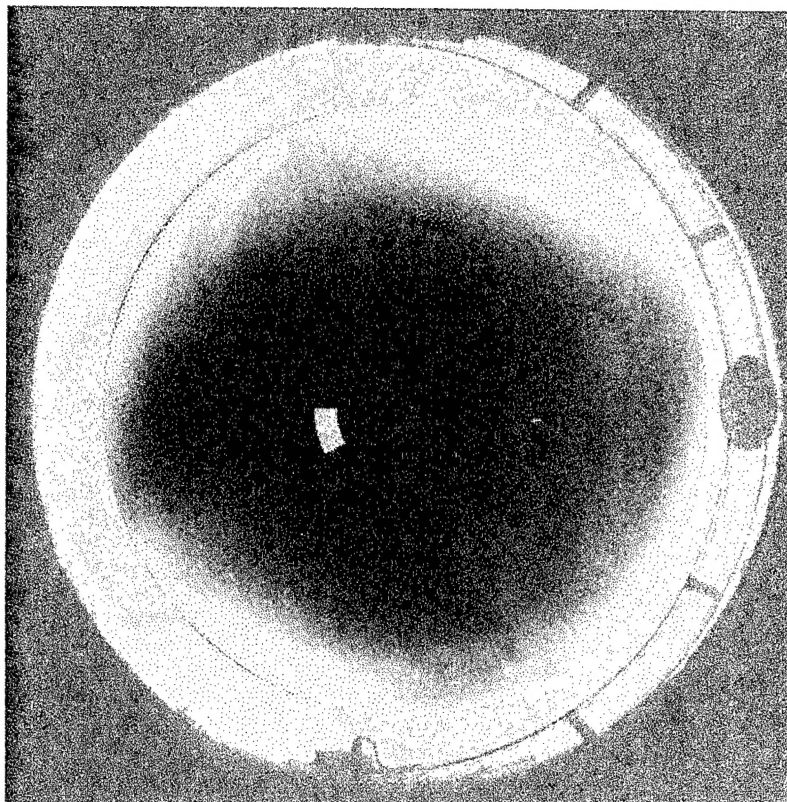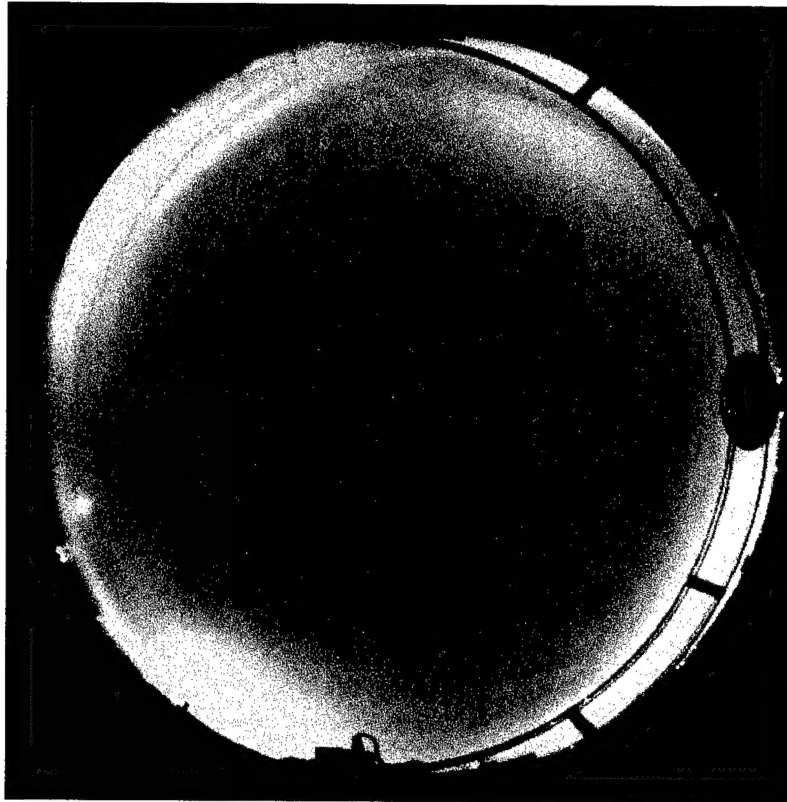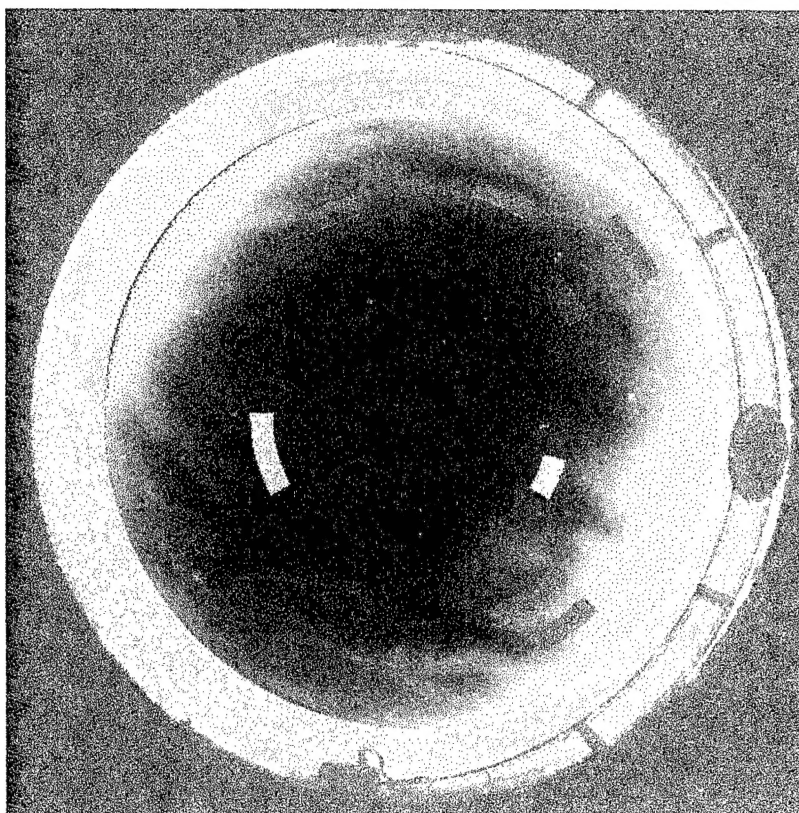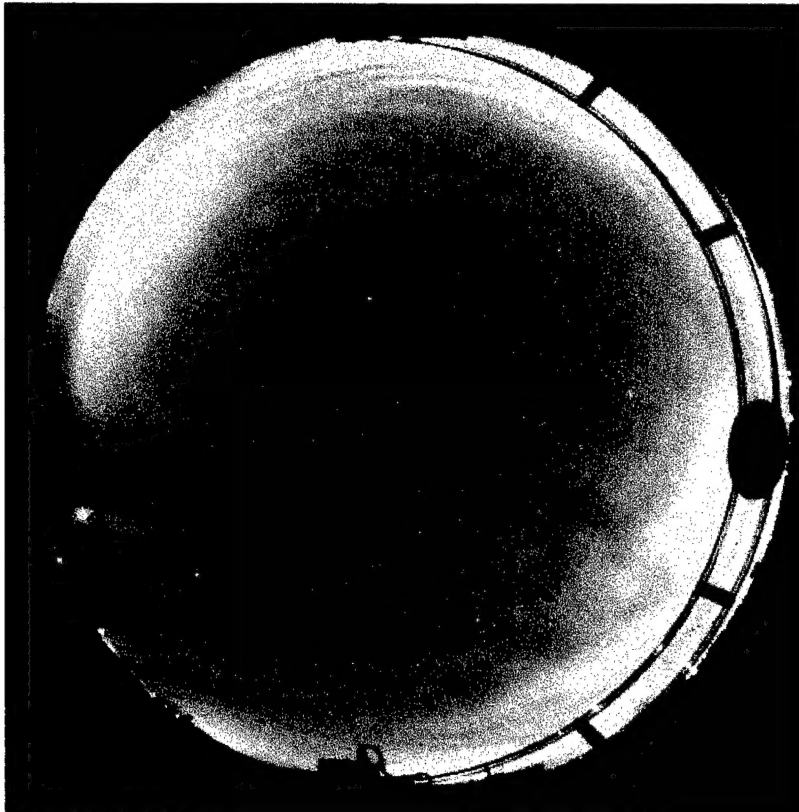Figure 8. Partly–Cloudy Scene
Grey = No Stars, Red = >50% Failure, Blue = <50% Failure

ONR/MPL REPORT DISTRIBUTION

Office of Naval Research   (3)
Department of the Navy
Ballston Tower One
800 North Quincy Street
Arlington, VA 22217-5660
      Atten: CDR Scott Tilden, ONR

Regional Director   (1)
ONR Detachment
San Diego Regional Office
4520 Executive Drive, Suite 300
San Diego, CA 92121-3019

Commanding Officer   (1)
Naval Research Laboratory
4555 Overlook Avenue, S.W.
Attn: Code 2627
Washington, D.C. 20375-5320

Defense Technical Information Center   (4)
8725 John J. Kingman Road
Suite 0944
Ft. Belvoir, VA 22060-6218